Supporting Information

Ferdous et al. 10.1073/pnas.1107341108

Materials and Methods

Mouse and Embryo Isolations. *FoxO1* knockout mice were described previously (1). *FoxO1* heterozygous males were backcrossed three times with wild-type (WT) FVB/n females, and tail DNA was used for genotyping. *FoxO1* heterozygous male and female progeny that were Cre negative were then intercrossed to isolate embryos at distinct developmental stages as described (2). The staging of embryos was performed by counting the presence of a vaginal plug as day 0.5 after conception and by counting the number of somites. Genomic DNA, extracted either from yolk sacs or embryo proper, was used for genotyping as described (2). *FoxO1*-WT and -null littermates were used in each experiment. Isolated embryos were photographed before or after fixation in 4% paraformadehyde (PFA) using either Openlab 4.0.1 acquisition software and a Zeiss Axiocam digital CCD camera or an MZ6 microscope (Leica), interfaced with a Macintosh G4 computer. In some cases, embryos were photographed without detaching the allantois from the placenta. *FoxO1*-WT and -null littermates at each developmental stage were photographed under identical conditions and magnification. Embryos at different developmental stages were photographed at different magnifications to fill the frame. All mice were maintained in the animal facility at University of Texas Southwestern Medical Center according to the guidelines of the institutional animal care and use committee and the Animal Resource Center.

Histological and Immunohistochemical Analyses. All embryos were harvested in ice-cold PBS, fixed in PFA overnight at 4 °C, and then processed as described (2). In some cases, embryos within deciduae were fixed in 4% PFA overnight at room temperature and then processed. Immunostaining for α-endomucin, an endothelium-specific sialomucin, was performed according to previously published methods (2, 3). Briefly, sections were deparaffinized before permeabilization with Triton, quenched for endogenous peroxidase, blocked with normal goat serum, and incubated overnight at 4 °C with rat anti-endomucin antibody. Bound primary antibody was detected with biotinylated rabbit anti-rat IgG, peroxidase-streptavidin, and 3,3′-diaminobenzidine (DAB) chromagen. Specimens were subsequently dehydrated and cleared before coverslipping with permount.

Immunostaining was performed for Ki67 (Novocastra; VP-K452), a cell cycle-associated protein expressed from G1 through the end of M phase, as described (2). Briefly, sections were deparaffinized, quenched for autofluorescence after antigen retrieval, blocked with mouse-on-mouse (MOM) IgG blocking reagent (Vector Laboratories) and incubated overnight at 4 °C with Novocastra (Vector) anti-Ki67 antibody. Bound primary antibody was detected with MOM biotinylated antimouse IgG and fluorescein-avidin DCS. Specimens were subsequently coverslipped with Vectashield mounting medium.

Immunostaining for FoxO1 was performed on a paraffin section adjacent to that stained with Vcam-1 (described in the main text, Fig. 4*C*). Following deparaffinization and citrate buffer microwave antigen retrieval, the section was exposed to FoxO1 rabbit polyclonal antisera (Cell Signaling; no. C29H4) at a dilution of 1:1,350 in PBS. Bound primary antibody was amplified and detected as described for Vcam-1. Vcam-1 and FoxO1 sections were visualized under 10× objective magnification with bright-field illumination, and carefully aligned before monochromatic CCD imaging (Zeiss Axioplan 2iE/Axiocam). Using Adobe Photoshop CS2, resulting images were inverted and levels adjusted to yield saturated immunostain as white over negative black background. FoxO1 and Vcam-1 signals were pseudocolored red and green, respectively, and merged.

Chromatin Immunopreciptation (ChIP) Assay. ChIP assays for evaluating *VCAM1* promoter binding of FoxO1 were performed as previously described (2, 4, 5). Briefly, C2C12 myoblast cells were transfected with 10 μg myc-tagged ca-FoxO1 vector (6) in a 15-cm culture dish. Formaldehyde (1% final concentration) was added 24 h following transfection and chromatin solution was prepared by sonication. Immunoprecipitation reactions were carried out using an anti-myc (Cell Signaling) and control IgG sera. Promoter occupancy of FoxO1 was analyzed by amplifying the DNA fragment (288 bp) corresponding to upstream FREs (Fig. S7*A*) using the following set of primers (forward: 5′-CCCTTCATTCTGCATCAACGTCC-3′ and reverse: 5′-GTGACAGCAAAGACAGAGATCACTC-3′). Genomic DNA isolated before immunoprecipitation was diluted 30- and 100-fold. Diluted DNA (1 μL), indicated as input, and immunoprecipitated DNA (1 and 3 μL) were used for the PCR.

RT-PCR and Quantitative RT-PCR Analyses. Total RNA from *FoxO1*-WT and -null embryos and extraembryonic tissue, yolk sac was extracted using TRIzol (Invitrogen) according to the manufacturer's instructions. Equal amounts (0.5 μg) of total RNA were used to prepare cDNA and used for quantitative RT-PCR (qRT-PCR) analyses for endothelial-specific genes as described previously (2). Total RNA was also extracted from *FoxO1*-WT and -null hearts and allantois, and equal amounts (0.35 μg) of RNA were used to prepare cDNA using iScript cDNA synthesis kit according to manufacturer's instructions (Bio-Rad). To prepare cDNA from endothelial progenitor cells, we extracted and amplified RNA from Tie2-GFP$^+$ cells isolated from E9.0 Tie2-GFP embryo as described (2). cDNA was diluted four to five times and used for qRT-PCR analyses of genes using gene-specific Taqman probes where 18S RNA was used as a loading control. In addition, cDNA of *FoxO1*-WT and -null embryos and allantois was used for RT-PCR analysis of *FoxO1* using forward (5′-ATCACCAAGGCCATCGAGAGC-3′) and reverse (5′-ACTGTTGTTGTCCATGGACGC-3′) primer sets, as described previously (2).

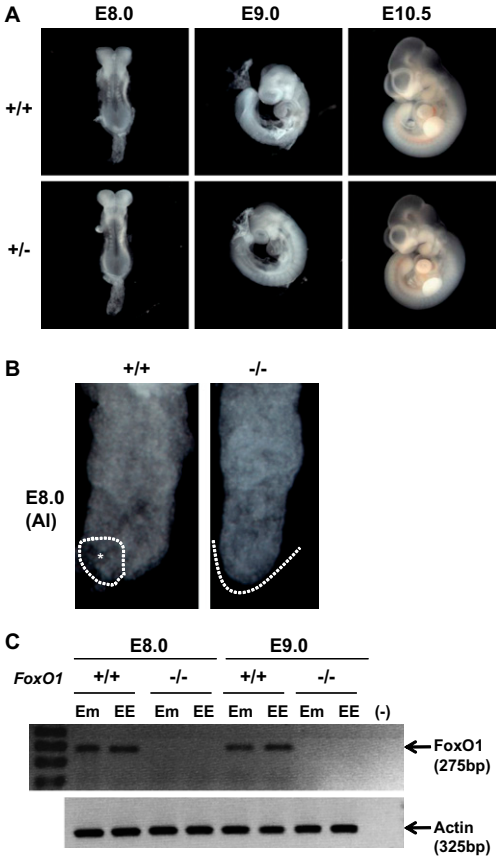

Fig. S1. Embryonic development of *FoxO1*-heterozygous mice is normal. (*A*) Morphological appearances of *FoxO1*-WT (+/+) and -heterozygous (+/–) embryos isolated at the indicated developmental stages. Note that WT and heterozygous littermates are morphologically indistinguishable at each developmental stage. (*B*) An enlarged view of *FoxO1*- WT (+/+) and -null (–/–) allantois at E8.0 reveals open (asterisk in dotted circle) and closed (dotted line) configurations, respectively. (*C*) RT-PCR analyses demonstrated *FoxO1* gene expression in *FoxO1*-WT (+/+), but not in -null (–/–), embryonic (Em) and extraembryonic (EE) tissues at the indicated developmental stages. The lengths of *FoxO1* and α-*actin* (as control) amplicons are indicated in base pairs (bp).

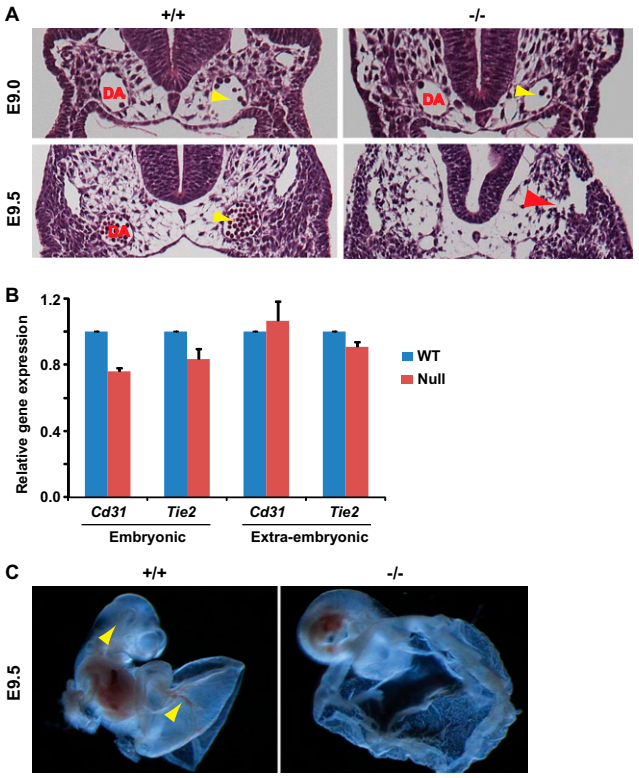

Fig. S2. Embryonic and extraembryonic vascular developments are normal in early developing *FoxO1*-null mice. (*A*) Enlarged views of dorsal aorta (DA) of *FoxO1*-WT (+/+) and -null (–/–) embryos at the indicated developmental stages are shown (also Fig. 1*B*). The presence of erythrocytes within DA in both E9.0 and E9.5 of *FoxO1*-WT (+/+) embryos is indicated (yellow arrowheads). Note the presence of erythrocytes within DA at E9.0 (yellow arrowhead), but not at E9.5, of *FoxO1*-null (–/–) embryos. Red arrowhead indicates a disrupted vessel in null mice. (*B*) Quantitative RT-PCR analyses of the endothelial-specific genes, *CD31* and *Tie2*, expression in E8.5 WT and *FoxO1*-null embryo proper (embryonic) and extra embryonic (i.e., yolk sac) is shown. Note that embryonic and extra-embryonic expression of both genes was essentially similar in both genotypes. (*C*) *FoxO1*-WT (+/+) and -null (–/–) littermates isolated at E9.5 without separating from yolk sac (YS). Note that the well-developed YS and head vasculatures (yellow arrowheads) in *FoxO1*-WT embryo is absent in null littermates.

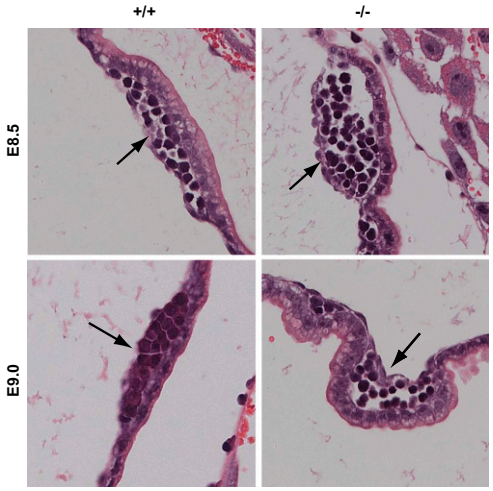

Fig. S3. Blood island formation is normal in early developing *FoxO1*-null mice. Higher magnification of the boxed area of Fig. 2*B* reveals normal blood island (arrows) formation in WT (+/+) and *FoxO1* null (–/–) embryos at the indicated developmental stages.

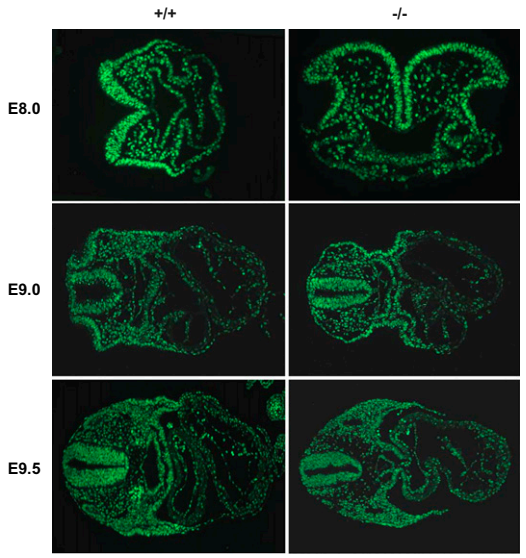

Fig. S4. Active cellular proliferation was not altered in the *FoxO1*-null embryo. Immunohistochemical analyses for Ki67 were used to detect proliferating cells in WT (+/+) and *FoxO1* null (–/–) embryos at the indicated developmental stages. Note that compared with WT littermates, no significant proliferative defects were observed in *FoxO1*-null embryos.

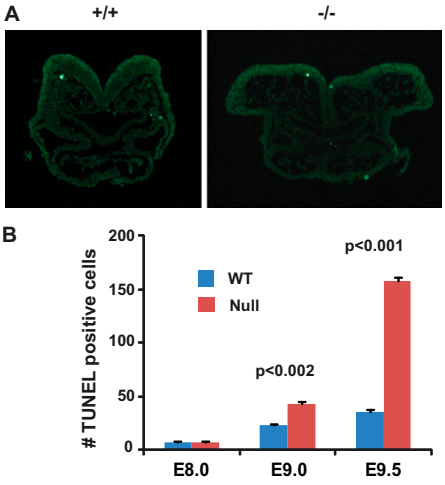

Fig. S5. Progressive apoptotic cell death in *FoxO1*-deficient embryos. (*A*) TUNEL assays indicated that, compared with *FoxO1*-WT (+/+) littermates, absence of FoxO1 did not promote widespread apoptosis in *FoxO1* null (–/–) embryo at E8.0. (*B*) Quantification of TUNEL-positive cells in embryo proper of WT (+/+) and *FoxO1* null (–/–) mice at the indicated developmental stages ($n = 3$). Note an age-dependent and progressive induction of apoptotic cell death in *FoxO1*-null (–/–) embryos. Error bars represents mean ± SD and *P* values were calculated by Student's *t* test.

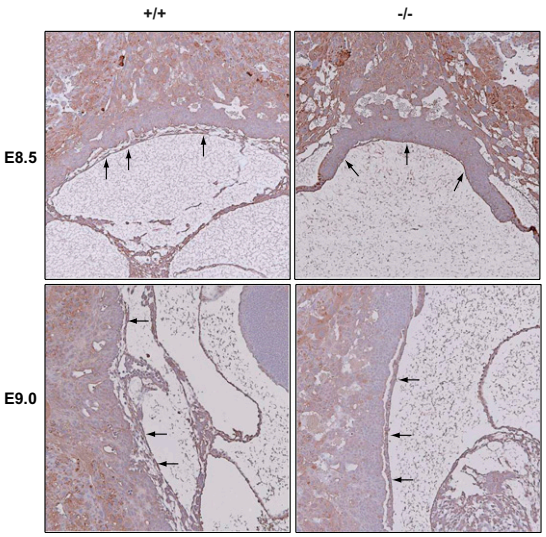

Fig. S6. α4 integrin expression was not altered in *FoxO1*-null embryo. Immunohistochemical analyses for α4 integrin in the chorion of WT (+/+) and *FoxO1*-null (–/–) embryos at the indicated developmental stages. Note that α4 integrin expression (arrows) was similar in both genotypes.

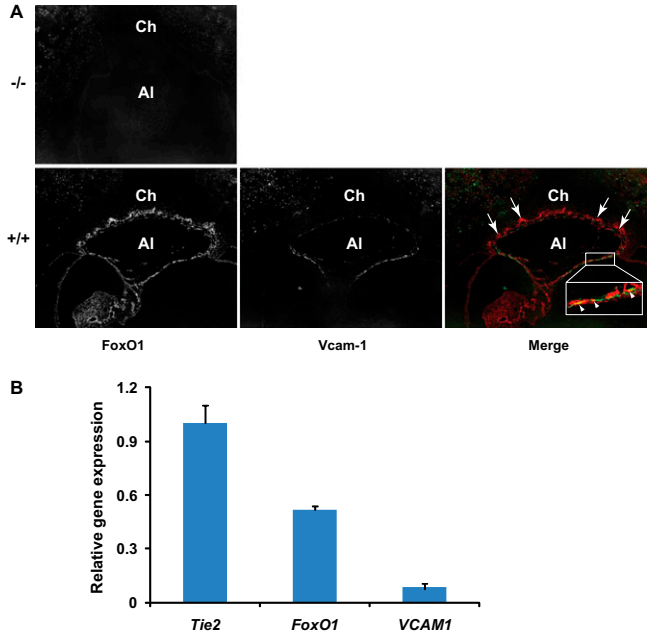

Fig. S7. *FoxO1* and *VCAM1* reveal similar expression pattern in allantois of developing embryos. (*A*) Allantois (Al) of E8.5 *FoxO1*-WT (+/+) and -null (–/–) embryos within deciduas were immunostained for FoxO1. Note that FoxO1 was undetectable in *FoxO1*-null allantois. An adjacent section of *FoxO1*-WT was also immunostained for Vcam-1, and both FoxO1 and Vcam-1 sections were visualized under 10× objective magnification with bright-field illumination. Following alignment, FoxO1 (red) and Vcam-1 (green) signals were pseudocolored and merged (yellow, arrowheads). Note that FoxO1 and Vcam-1 reveal an essentially similar pattern of expression in developing allantois; FoxO1 expression in the chorionic (Ch) plate is indicated (arrows). (*B*) Coexpression of *FoxO1* and *VCAM1* in endothelial progenitor cells of developing embryos was evaluated in Tie2-GFP$^+$ cells, isolated from E9.0 Tie2-GFP embryos using FACS as described previously (2). Purified RNA was amplified and used for qRT-PCR analyses of *Tie2*, *FoxO1*, and *VCAM1* genes. *Tie2* expression was normalized to 1 and the relative expression of *FoxO1* and *VCAM1* is indicated. Note that *FoxO1* and *VCAM1* genes were expressed in the endothelial progenitor cells and the *VCAM1* message was less abundant than *FoxO1*.

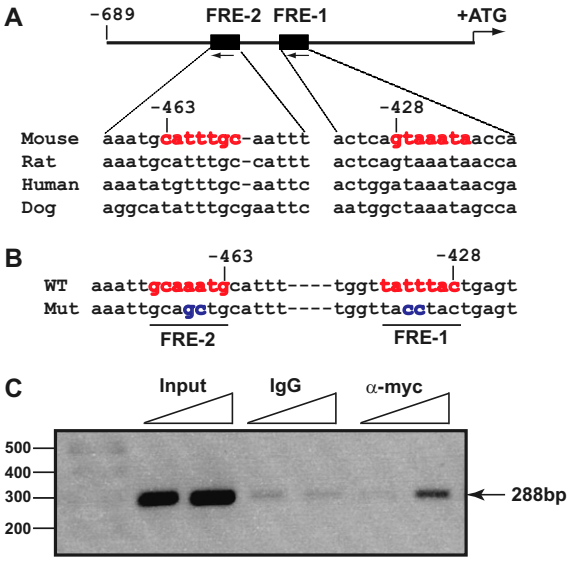

Fig. S8. The upstream promoter region of the *VCAM1* gene harbors conserved FoxO-responsive elements (FREs). (*A*) Schematic alignment of mouse, rat, human, and dog *VCAM1* upstream promoter regions harboring two FREs is shown. Nucleotide sequences of FREs in reverse orientation (arrows under the black box) are indicated in red. Numbers indicate the position upstream from the translation initiation site (+ATG). (*B*) Schematic alignment of nucleotide sequences for wild type (WT) and mutated (mut) FREs (underlined), used for reporter assays (Fig. 3*D*). Mutated nucleotides are indicated in blue. (*C*) ChIP assays reveal FoxO1 occupancy of the *VCAM1* promoter in vivo. Chromatin solution prepared from C2C12 myoblasts transfected with myc-tagged caFoxO1-expressing vector was immunoprecipitated with anti-myc and control IgG sera. Note that the *VCAM1* promoter harboring the FREs amplified (arrow) only from DNA immunoprecipitated with anti-myc, but not IgG, serum. DNA isolated without immunoprecipitation was used as input.

1. Paik JH, et al. (2007) FoxOs are lineage-restricted redundant tumor suppressors and regulate endothelial cell homeostasis. *Cell* 128:309–323.
2. Ferdous A, et al. (2009) Nkx2-5 transactivates the Ets-related protein 71 gene and specifies an endothelial/endocardial fate in the developing embryo. *Proc Natl Acad Sci USA* 106: 814–819.
3. Brachtendorf G, et al. (2001) Early expression of endomucin on endothelium of the mouse embryo and on putative hematopoietic clusters in the dorsal aorta. *Dev Dyn* 222:410–419.
4. Ferdous A, et al. (2007) The role of the proteasomal ATPases and activator monoubiquitylation in regulating Gal4 binding to promoters. *Genes Dev* 21:112–123.
5. Caprioli A, et al. (2011) Nkx2-5 represses Gata1 gene expression and modulates the cellular fate of cardiac progenitors during embryogenesis. *Circulation* 123:1633–1641.
6. Kitamura T, et al. (2007) A Foxo/Notch pathway controls myogenic differentiation and fiber type specification. *J Clin Invest* 117:2477–2485.